

**Tip-functionalized carbon nanotubes under electric fields**Changwook Kim,\* Kwanyong Seo, and Bongsoo Kim<sup>†</sup>*Department of Chemistry, Korea Advanced Institute of Science and Technology, Daejeon 305-701, Republic of Korea*

Noejung Park

*Research Organization for Information Science and Technology, 2-2-54 Naka-Meguro, Meguro-ku, Tokyo 153-0061, Japan*Yong Soo Choi, Kyung Ah Park, and Young Hee Lee<sup>‡</sup>*Center for Nanotubes and Nanostructured Composites, Institute of Basic Science, Department of Physics, Sungkyunkwan University, Suwon 440-746, Republic of Korea*

(Received 6 May 2003; published 5 September 2003)

We investigated the electronic structures of chemically modified carbon nanotube tips under electric fields using density functional calculations. Hydrogen, oxygen, and hydroxyl group-terminated nanotubes have been considered as field emitters or probe tips. In the case of the open-ended tubes, the field emission originates primarily from the dangling-bond states localized at the edge, whereas the pentagonal defects are the main source of the field emission in the capped tubes. The open-ended nanotube with a zigzag edge is an efficient field emitter because of the localized electronic states around the Fermi level and the atomic alignment of carbon-carbon bonds along with external electric fields. Tip functionalization alters the local density of states as well as the chemical selectivity of nanotubes in various ways. The correlations between atomic geometries of chemically functionalized tips and their electronic structures are further discussed. We propose that a hydrogen-terminated tube would be a promising probe tip for selective chemical imaging.

DOI: 10.1103/PhysRevB.68.115403

PACS number(s): 61.46.+w, 73.22.-f, 79.70.+q

**I. INTRODUCTION**

Carbon nanotubes (CNT's) are suitable materials for field emitters because of their unique electronic and atomic structures with high aspect ratio.<sup>1</sup> In addition, remarkable emission stability<sup>2,3</sup> and mechanical stiffness<sup>4</sup> make CNT's one of the promising candidates for use as tip materials in electronic applications. They have been recently applied to the cathode tips in the field emission display (FED) devices<sup>5</sup> and the probe tips in surface-analysis instruments.<sup>6,7</sup>

The scanning tunneling microscope (STM) is based on vacuum tunneling phenomenon and is a powerful tool to study both the geometrical and electronic structures of surfaces.<sup>8</sup> The CNT tips in a STM probe have a smaller effective diameter than conventional tips, and provide an improved resolution in the imaging of nanostructures. Chemical functionalization of the STM probe tips is also an attractive method for recognizing specific chemical species in STM images. For example, the oxygen atoms on the ether molecule adsorbed on a surface were selectively observed by STM with a carboxyl-terminated CNT tip, which is due to electron tunneling through the hydrogen bonding between the ether oxygen atoms and hydrogen atoms in carboxyl group of the CNT tip.<sup>9</sup>

Tip functionalization of CNT's can be manipulated by several methods. The oxidative purification process terminates open ends of single-walled carbon nanotubes (SWNT's) with hydroxyl (OH) or carboxylic (COOH) groups.<sup>10,11</sup> These carboxylic groups can be converted into various types of functional groups such as amides or esters by reaction with other reagents.<sup>12</sup> Functionalization using a simple gas-phase reaction is also possible. Wong *et al.* have demonstrated that the end of CNT probe tips can be modified

using various gases (H<sub>2</sub>, O<sub>2</sub>, and N<sub>2</sub>) after activation with a momentary arc discharge created at the tips.<sup>13</sup> In spite of many experimental observations on the CNT functionalization, these systems are not clearly understood yet due to the absence of a reliable theoretical model.

Since the electrons are mainly emitted from the end of the tips,<sup>14</sup> it is important to understand the field emission characteristics<sup>15</sup> at the edge of CNT's. The field emission is sensitively dependent on the adsorbates<sup>16-19</sup> and the edge structures.<sup>20-27</sup> Tip functionalization changes the local density of states around the Fermi level, thus affecting the tunneling current. This chemical modification of the CNT tip is also desirable for the application of molecular-scale sensing using chemical selectivity. Little is known, however, about the relationship between the electronic structures of the chemically modified tips and their field emission properties. Understanding the field emission mechanism would be useful for designing efficient field emitters and functional probes.

In this report, we present density functional calculations for the electronic structures of the bare and functionalized CNT edges under electric fields. The capped and open-ended tubes are considered as representative field emitters, and the chemically modified tubes are modeled for probe tips. We find that the topological defects and dangling bonds play an important role in the field emission. The open-ended zigzag CNT enhances the field emission due to both electronic and geometrical factors. Tip functionalization not only modifies the electronic structures at the CNT edge but also changes the chemical selectivity of the CNT's. In functionalized CNT's, the sharp and localized states near the Fermi level could act as the available states of tunneling electrons.

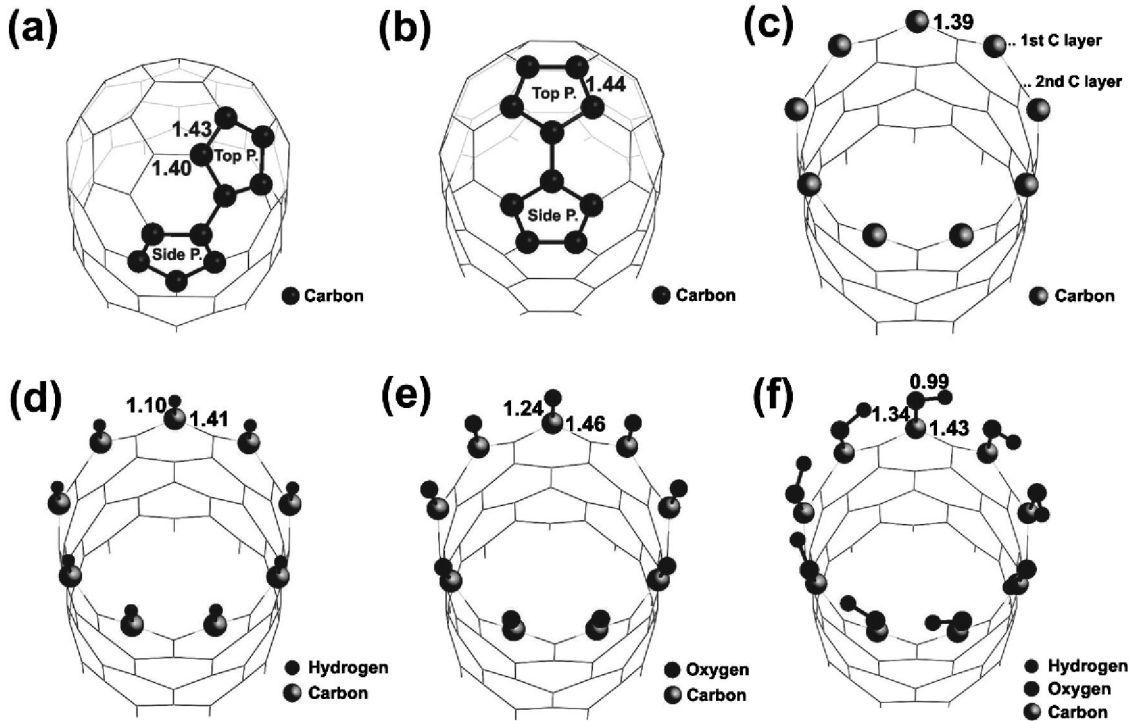


FIG. 1. Optimized geometries of the (a) capped (9,0) tube, (b) capped (5,5) tube, (c) open-ended (9,0) tube, (d) hydrogen-terminated tube, (e) oxygen-terminated tube, and (f) hydroxyl-terminated tube by the LDA calculation. These figures are presented in a perspective view of  $15^\circ$ . All bond lengths are in units of  $\text{\AA}$ .

## II. THEORETICAL APPROACHES

We considered five types of edge structures based on single-walled zigzag (9,0) and armchair (5,5) nanotubes, as shown in Fig. 1. The diameters of the zigzag and armchair nanotubes are 7.0 and 6.8  $\text{\AA}$ , respectively, and the average bond length is 1.42  $\text{\AA}$ . Supercells of eight and ten layers of carbon rings along the tube axis ( $z$  axis) are used, respectively,<sup>28</sup> where the bottom dangling bonds are saturated by hydrogen atoms in order to emulate the bulk properties.

Our total energy calculations and corresponding structure optimizations are based on the density functional formalism within the local density approximation (LDA) and the generalized gradient approximation (GGA).<sup>29</sup> The exchange-correlation energy in the LDA is parametrized by the Perdew-Wang scheme<sup>30</sup> and Becke's corrected exchange functional<sup>31</sup> is adopted in the GGA. All-electron Kohn-Sham wave functions are expanded in a local atomic orbital basis set with each basis function defined numerically on an atomic-centered spherical-polar mesh. We used a double numeric polarized basis set. In this basis set, the  $2s$  and  $2p$  carbon orbitals are represented by two wave functions each, and a  $3d(2p)$  type wave function on each carbon (hydrogen) atom is used to describe the polarization. No frozen core approximation is used throughout the calculations. For accurate binding energy calculations, GGA calculations are performed after geometrical optimization by the LDA. The forces on each atom to be converged during each relaxation are less than  $10^{-3}$  a.u.

The local density of states at the nanotube tip under the

electric field is calculated with much longer nanotubes ( $\sim 30$   $\text{\AA}$ , 250–280 atoms). According to a previous study,<sup>21</sup> the induced local field converges to the experimental value as the tube length is increased over 30  $\text{\AA}$ . Therefore, the relaxed geometry of the nanotube body is attached to the optimized geometry of the finite tube to investigate the properties of the tube edges more realistically. We also applied a uniform external electric field to the elongated tube axis (parallel to the  $z$  axis). The standard pseudopotential method is employed and the external electric field ( $E_{\text{ext}}z$ ) is described accurately by a self-consistent iteration.<sup>32</sup> The Hamiltonian is composed of the potential of the external field, kinetic operator  $T$ , Hartree ( $V_H$ ), and exchange-correlation ( $V_{\text{xc}}$ ) potential evaluated from the LDA.

$$H = T + V_H + V_{\text{xc}} - eE_{\text{ext}}z. \quad (1)$$

In this case, the minimal basis set is used to reduce the computational cost and the Troullier-Martins pseudopotentials<sup>33</sup> with a cutoff energy of 40 Ry are employed for the description of atomic potentials.

## III. RESULTS AND DISCUSSION

Various edge structures are considered in this study in order to investigate the field emission properties of CNT's at the end of the tip. Figures 1(a) and 1(b) show capped geometries at the tip with a hemisphere of  $C_{60}$  having pentagons. The zigzag (9,0) tube has a hexagon at the top of the cap surrounded by alternating three pentagons and three hexagons, whereas the armchair (5,5) tube has a pentagon at the

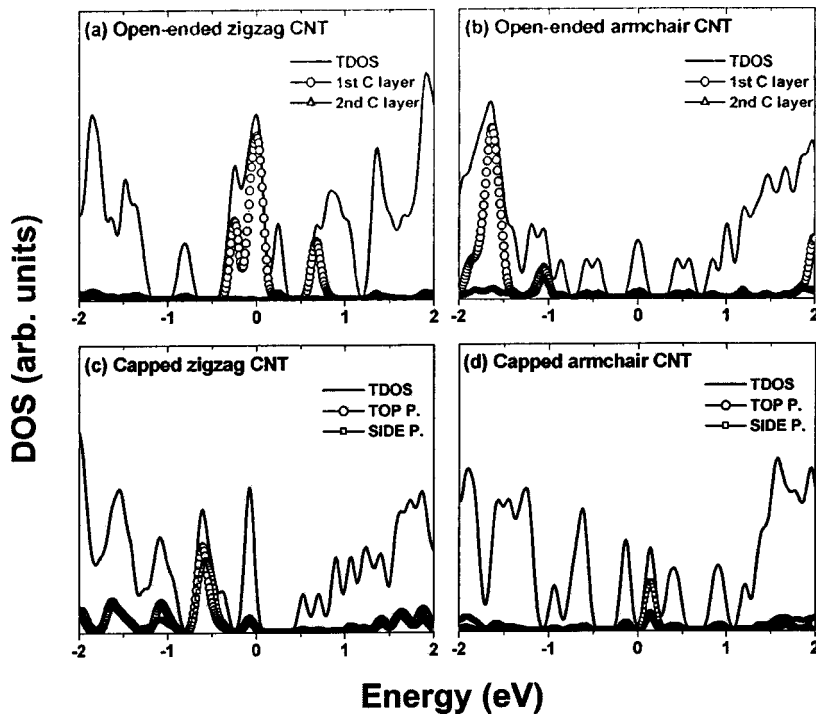


FIG. 2. The electronic total density of states (TDOS) and the local density of states (LDOS) for the (a) open-ended (9,0) zigzag tube, (b) open-ended (5,5) armchair tube, (c) capped (9,0) zigzag tube, and (d) capped (5,5) armchair tube with an electric field of  $0.5 \text{ V/\AA}$ . The solid line indicates the TDOS of nanotubes, and the other marked lines represent the LDOS from the top or side pentagons at the cap in the case of a capped nanotube and from the topmost first layer or second layer at the edge in the case of an open-ended nanotube. The Fermi level is set to zero in all figures.

top of the cap surrounded by five hexagons. These (9,0) and (5,5) tubes have additional three and five pentagons at the side of the cap, respectively [Figs. 1(a) and 1(b)]. The optimized geometry of a capped (9,0) tube has alternating bond lengths of 1.40 and 1.43  $\text{\AA}$  at a top hexagon, whereas the capped (5,5) tube has equivalent bond lengths of 1.44  $\text{\AA}$  at the top pentagon. These pentagons at the cap are topological defects in a curved hexagonal lattice<sup>34</sup> and play an important role in the field emission.<sup>35,36</sup>

Figure 1(c) shows an open-ended (9,0) tube, where the dangling bonds remain unsaturated. This (9,0) tube belongs to the  $D_{9d}$  point group with nine edge atoms, whereas an open-ended (5,5) tube (not shown in the figures) has  $D_{5d}$  symmetry with ten edge atoms. The unpaired electrons at the edge of a zigzag nanotube attempt to establish a double bond with their neighbors, resulting in a bond length of 1.39  $\text{\AA}$ . In an armchair tube, on the other hand, all atoms at the edge are tetravalent and strongly bound through triple bonds, resulting in a lower edge energy of 0.79 eV per edge atom than in a zigzag tube.<sup>37</sup> These calculations suggest that a zigzag tube edge is more reactive with adsorbates than armchair and capped tube edges are.

In other geometries of (9,0) CNT's, the dangling bonds are chemically terminated by hydrogen atoms (H), oxygen atoms (O), and hydroxyl groups (OH), respectively [Figs. 1(d)–1(f)]. These chemical terminations are similar to the case of gas adsorption on a tube edge, as demonstrated in the previous report.<sup>16</sup> For the H-terminated CNT, hydrogen atoms saturate the dangling bonds of the tube, and the CNT recovers a complete  $sp^2$  bonding character without appreciable structural distortion at the tube edge. The edge structure is slightly modified, however, in an O-terminated CNT due to repulsive forces between oxygen atoms that are attributed to significant amount of charge transfer from carbon atoms to oxygen atoms. The C-C back bonds in the CNT are

extended to 1.46  $\text{\AA}$ , and oxygen atoms are tilted towards the radial direction of tube. In case of the OH-terminated CNT [Fig. 1(f)], hydroxyl groups are oriented along the circumference of the tube edge because of the hydrogen bonding between the hydrogen atom and the next oxygen atom. These functional groups at tube edges have relatively large adsorption energies, which are greater than  $-5 \text{ eV}$ , and therefore are very stable in ambient environment.<sup>16</sup>

Figure 2 shows the local density of states (LDOS) at the edge of nanotube under an electric field of  $0.5 \text{ V/\AA}$ . A large peak of the open-ended zigzag tube near the Fermi level, as presented in Fig. 2(a), originates from the dangling bonds of the topmost carbon layer at the edge.<sup>20,21</sup> This sharply localized state is also observed in zigzag edges of nanographite ribbons, which may be related to spin polarization.<sup>38</sup> In the case of an open-ended armchair tube in Fig. 2(b), the stable nature of triple bonds shifts the edge states to the deep valence band at  $-1.6 \text{ eV}$  below the Fermi level. The contribution to the LDOS at the Fermi level is negligible, in good contrast with an open-ended zigzag tube in Fig. 2(a). We find that the DOS's at the Fermi level are equally contributed from all carbon atoms in the tube wall, suggesting that the peak at the Fermi level originates from the metallic nature of armchair tubes.<sup>39</sup> The finite DOS at the Fermi level corresponds to the  $\pi$  and  $\pi^*$  bands in an infinite nanotube. On the other hand, in the capped zigzag tube, the peak at  $-0.7 \text{ eV}$  below the Fermi level in Fig. 2(c), comes from pentagons at the top and side of the cap.<sup>35</sup> In the case of a capped armchair tube, the peak originating from the pentagons is located at  $0.2 \text{ eV}$  above the Fermi level, as shown in Fig. 2(d). In this case, DOS's at the Fermi level disappear by the presence of the cap, in contrast with the case of an open-ended armchair tube, as shown in Fig. 2(b), which has DOS's at the Fermi level. The LDOS's, as shown in Figs. 2(c) and 2(d), indicate

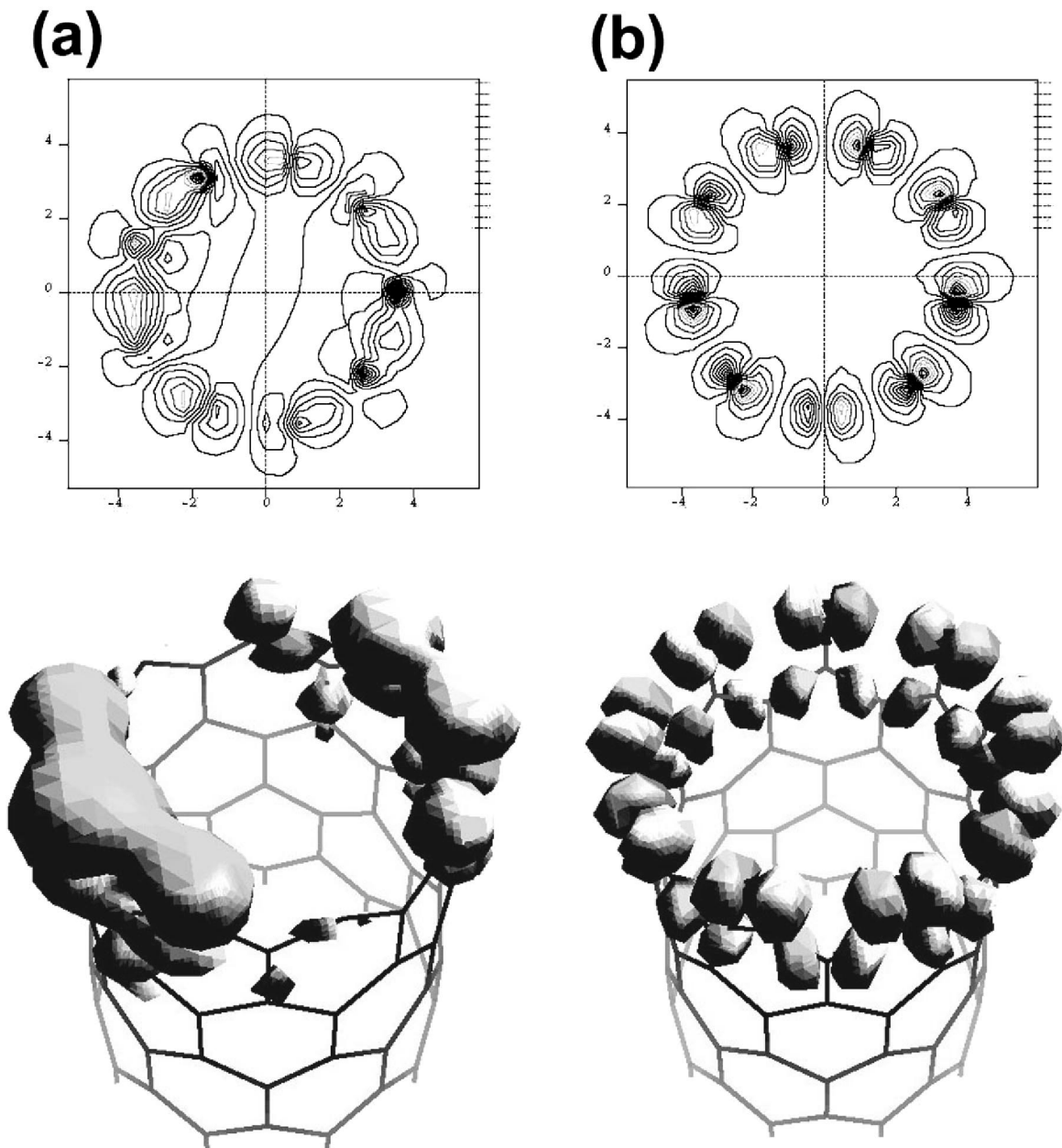


FIG. 3. The local charge densities of the (a) open-ended (9,0) tube and (b) oxygen-terminated (9,0) tube at the highest occupied molecular orbital (HOMO) under an electric field of  $0.5 \text{ V/\AA}$ . These figures are presented in a perspective view of  $15^\circ$ . The contour plots are demonstrated at the topmost atoms within the (001) plane.

that the position of the LDOS peak depends sensitively on the relative location of pentagons at the cap.<sup>35</sup> The capped (5,5) armchair tube has one top pentagon and five side pentagons, giving the peak position above the Fermi level, whereas the capped (9,0) zigzag tube has three top pentagons and three side pentagons at the cap, giving the peak position below the Fermi level. The relative position of the LDOS in this case may also depend on the external field strength.<sup>22</sup>

We assumed that only electronic states within a narrow energy window near the Fermi level could contribute to the low-temperature electron field emission, and calculated the integrated local density of states from  $-2 \text{ eV}$  to the Fermi level in Fig. 2, which would represent the emission probab-

ity of electrons at the end region of nanotubes.<sup>23</sup> The calculated values are summarized in Table I. The tunneling probability is higher in open-ended tubes than in capped tubes. Thus the field emission current in the open-ended tubes is

TABLE I. Calculated number of electrons per edge atom resulted from integrating localized electronic density of states between the  $-2 \text{ eV}$  and the Fermi level.

Electron/atom	Zigzag (9,0) tube	Armchair (5,5) tube
Open-ended tube	0.678	0.657
Capped tube	0.221	0.0358

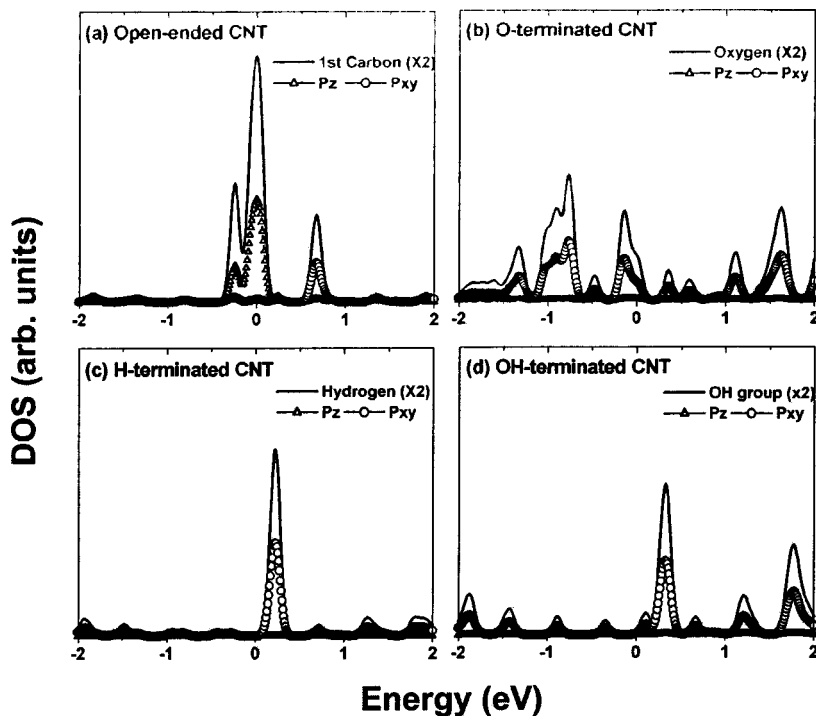


FIG. 4. The electronic local density of states (LDOS) for (a) topmost carbon atoms in an open-ended tube, (b) oxygen atoms in an O-terminated tube, (c) hydrogen atoms in an H-terminated tube, and (d) hydroxyl group (OH) in an OH-terminated tube. The solid lines indicate the LDOS and other marked lines represent the  $p$  orbital components [open triangles ( $\Delta$ ) for  $p_z$  and open circles ( $\circ$ ) for  $p_{xy}$ ] resolved from the LDOS. The Fermi level is set to zero in all figures.

enhanced, in good agreement with experiments<sup>40,41</sup> and theoretical reports<sup>22,23,27</sup> from other groups. In addition, Table I shows that the nanotube with a zigzag edge is a more efficient field emitter than those with an armchair edge.<sup>21,22,27</sup> As mentioned above, the edge energy of a zigzag tube is higher than that of an armchair tube. This implies that the electrons at a zigzag edge are relatively unstable and less bound. Thus, those electrons can be easily extracted from the nanotube. The geometrical effect is caused by different alignments of carbon-carbon bonds adjacent to edge atoms. The bond orbitals in a zigzag tube can be more polarized because they are aligned parallel to the external electric field direction, whereas those in an armchair tube are less polarized due to the tilting of carbon-carbon bonds by  $30^\circ$  from the field direction.<sup>37</sup>

The open-ended tube is more desirable for functionalization of the CNT edge because of the existence of reactive dangling bonds, particularly on a zigzag tube edge. Tip functionalization with simple molecules saturates the dangling bonds and affects the electronic structures of the CNT. Functionalization of the CNT at the sidewall of the tube also modifies its electronic structures.<sup>42</sup> Figure 3 shows the contour plots and the local charge densities of the open-ended and O-terminated tubes at the highest occupied molecular orbital (HOMO) under an electric field of  $0.5 \text{ V/\AA}$ . For an open-ended tube, localized charge densities originate from unpaired electrons of carbon atoms at the edge. The asymmetrical distribution of charge densities in the contour plot comes from the degeneracy with the first level from the HOMO (HOMO-1 level).<sup>36</sup> In an O-terminated tube, oxygen atoms saturate the dangling bonds at a tube edge, and form double bonds between oxygen and edge carbon atoms. Thus, the doubly coordinated edge carbons with unpaired electrons transform to fully coordinated, tetravalent carbon atoms, and the lobes of orbitals which originated from edge carbon at-

oms are reduced compared to an open-ended tube. On the other hand, the lobes from the  $p$  orbitals of oxygen atoms at the topmost edge are directed perpendicular to the tube axis (parallel to the  $xy$  plane), which is demonstrated in the local charge densities and the contour plot in Fig. 3(b), and supported by the LDOS in Fig. 4(b). The LDOS of the O-terminated tube near the Fermi level shows that peaks are mainly contributed from the  $p_{xy}$  orbitals. This could be one of the reasons why the reduction of emission current is observed in oxygen-adsorbed tubes.<sup>21,19</sup> The LDOS of the open-ended tube, however, clearly reveals that  $p_z$  orbitals are the main source of the LDOS peak at the Fermi level as shown in Fig. 4(a). We emphasize that the unpaired electrons coming from those  $p_z$  orbitals (and also  $s$  orbitals) are easily polarized by an electric field.<sup>21,26</sup>

The H- and OH-terminated tubes have sharp LDOS's located just above the Fermi level as shown in Figs. 4(c) and 4(d), whereas most oxygen peaks in the O-terminated tube are located below the Fermi level. These localized states could become available states for tunneling electrons. O-terminated tubes, for instance, can probe the lowest unoccupied molecular orbital (LUMO) of a given chemical species in STM measurements, whereas H- and OH-terminated tubes can detect the HOMO of the chemical species at the surface. This suggests that the electronic structures of a functionalized probe are closely related to those of a surface chemical species, providing a novel way to chemical sensing, although the peak position might depend on the field strength<sup>22</sup> and the direction of the bias potential.<sup>26</sup> The narrow energy distribution of the localized states particularly in the H- and OH-terminated tubes enables them to probe the images of surface molecules with high resolution.

Hydrogen functional group at the STM tip can be highly sensitive to oxygen atoms in the surface of samples because

they can form hydrogen bonding. Therefore, these modified CNT's could be used as probe tips for chemically sensitive imaging with high resolution. For solution phase probing, the H-terminated tube is more useful than the OH-terminated tube as probe tips. While the OH group is deprotonated and becomes ionized into  $O^-$  at high pH, the H-terminated tube is pH independent, and nonionizable<sup>13</sup> due to relatively strong bonds between the edge carbon atoms and hydrogen atoms.<sup>16</sup>

#### IV. SUMMARY

We investigated the field emission mechanism of bare and chemically modified CNT's. Tunneling properties of field emitters and probe tips were studied for various edge structures. According to the analysis of LDOS with electric fields, defects (pentagons or dangling bonds) are the main origin of the field emission. We found that the open-ended CNT with a zigzag edge is an efficient field emitter because of both the electronic and geometrical factors. Electronic states coming from the dangling bonds are localized around the Fermi

level, and increase the tunneling probability of electrons, resulting in an enhancement of field emission. In addition, the carbon-carbon bonds adjacent to edge atoms are aligned parallel to the external electric fields and facilitate polarization. Tip functionalization modifies the electronic states and the chemical selectivity of CNT tips. The sharp and localized states in the chemically modified CNT's provide available states for tunneling electrons and make them probe the images of a given chemical species with high resolution. The H-terminated tube is a nonionizable selective chemical imaging probe with improved resolution. This could become a desirable probe tip for selective chemical sensing.

#### ACKNOWLEDGMENTS

We thank the MOST for the National R&D Project for Nano Science and Technology, NRL program, KOSEF through CNNC, and BK21 program. We acknowledge the supercomputer center at Chonbuk National University for allowing us to use their computer.

\*Also with Technology division, Samsung SDI Co.,Ltd., Suwon, 442-390, Korea.

†Electronic address: bongsoo@kaist.ac.kr

‡Electronic address: leeyoung@skku.ac.kr

<sup>1</sup>W.A. de Heer, A. Chatelain, and D. Ugarte, *Science* **270**, 1179 (1995).

<sup>2</sup>K. Dean and B. Chalamala, *Appl. Phys. Lett.* **75**, 3017 (1999).

<sup>3</sup>S.T. Purcell, P. Vincent, C. Journet, and Vu Thien Binh, *Phys. Rev. Lett.* **88**, 105502 (2002); P. Vincent, S.T. Purcell, C. Journet, and Vu Thien Binh, *Phys. Rev. B* **66**, 075406 (2002).

<sup>4</sup>B.I. Yakobson and R.E. Smalley, *Am. Sci.* **85**, 324 (1997).

<sup>5</sup>D.-S. Chung *et al.*, *Appl. Phys. Lett.* **80**, 4045 (2002).

<sup>6</sup>H. Dai, J.H. Hafner, A.G. Rinzler, D.T. Colbert, and R.E. Smalley, *Nature (London)* **384**, 147 (1996).

<sup>7</sup>S.S. Wong, E. Joselevich, A.T. Woolley, C.L. Cheung, and C.M. Lieber, *Nature (London)* **394**, 52 (1998).

<sup>8</sup>V. Meunier, M.B. Nardelli, C. Roland, and J. Bernholc, *Phys. Rev. B* **64**, 195419 (2001); A. Rubio, *Appl. Phys. A: Mater. Sci. Process.* **68**, 275 (1999).

<sup>9</sup>T. Nishino, T. Ito, and Y. Umezawa, *Anal. Chem.* **74**, 4275 (2002).

<sup>10</sup>H. Hiura, T.W. Ebbesen, and K. Tanigaki, *Adv. Mater. (Weinheim, Ger.)* **7**, 275 (1995).

<sup>11</sup>J. Chen, M.A. Hamon, H. Hu, Y. Chen, A.M. Rao, P.C. Eklund, and R.C. Haddon, *Science* **282**, 95 (1998).

<sup>12</sup>A. Hirsch, *Angew. Chem., Int. Ed.* **41**, 1853 (2002).

<sup>13</sup>S.S. Wong, A.T. Woolley, E. Joselevich, and C.M. Lieber, *Chem. Phys. Lett.* **306**, 219 (1999).

<sup>14</sup>J. Cumings, A. Zettl, M.R. McCartney, and J.C.H. Spence, *Phys. Rev. Lett.* **88**, 056804 (2002); S. Han and J. Ihm, *Phys. Rev. B* **66**, R241402 (2002).

<sup>15</sup>J.-M. Bonard, H. Kind, T. Stöckli, and L.-O. Nilsson, *Solid-State Electron.* **45**, 893 (2001).

<sup>16</sup>C. Kim, Y.S. Choi, S.M. Lee, J.T. Park, B. Kim, and Y.H. Lee, *J. Am. Chem. Soc.* **124**, 9906 (2002).

<sup>17</sup>N. Park, S. Han, and J. Ihm, *Phys. Rev. B* **64**, 125401 (2001).

<sup>18</sup>A. Maiti, J. Andzelm, N. Tanpipat, and P. von Allmen, *Phys. Rev. Lett.* **87**, 155502 (2001).

<sup>19</sup>S.C. Lim, Y.C. Choi, H.J. Jeong, Y.M. Shin, K.H. An, D.J. Bae, Y.H. Lee, N.S. Lee, and J.M. Kim, *Adv. Mater.* **13**, 1563 (2001).

<sup>20</sup>A. De Vita, J.-Ch. Charlier, X. Blase, and R. Car, *Appl. Phys. A: Mater. Sci. Process.* **68**, 283 (1999).

<sup>21</sup>S. Han and J. Ihm, *Phys. Rev. B* **61**, 9986 (2000).

<sup>22</sup>Ch. Adessi and M. Devel, *Phys. Rev. B* **62**, R13 314 (2000); **65**, 075418 (2002).

<sup>23</sup>G. Zhou, W. Duan, and B. Gu, *Phys. Rev. Lett.* **87**, 095504 (2001); G. Zhou, W. Duan, B. Gu, and Y. Kawazoe, *Appl. Phys. Lett.* **80**, 1999 (2002).

<sup>24</sup>J. Luo, L.-M. Peng, Z.Q. Xue, and J.L. Wu, *Phys. Rev. B* **66**, 155407 (2002).

<sup>25</sup>A. Mayer, N.M. Miskovsky, and P.H. Cutler, *Appl. Phys. Lett.* **79**, 3338 (2001); *Phys. Rev. B* **65**, 195416 (2002).

<sup>26</sup>L. Lou, P. Nordlander, and R.E. Smalley, *Phys. Rev. B* **52**, 1429 (1995).

<sup>27</sup>K. Tada and K. Watanabe, *Phys. Rev. Lett.* **88**, 127601 (2002).

<sup>28</sup>We also tested the convergence of the total energy and charge density with a longer tube (for instance, with 12 layers for a zigzag, and 14 layers for an armchair tube) layers. Charge densities are slightly changed, but the symmetries were clearly conserved.

<sup>29</sup>We performed calculations using DMOL<sup>3</sup>, which is a registered software product of Molecular Simulations Inc.; B. Delley, *J. Chem. Phys.* **92**, 508 (1990); *J. Phys. Chem.* **100**, 6107 (1996).

<sup>30</sup>J.P. Perdew and Y. Wang, *Phys. Rev. B* **45**, 13 244 (1992).

<sup>31</sup>A.D. Becke, *J. Chem. Phys.* **88**, 2547 (1988).

<sup>32</sup>S. Han, M.H. Lee, and J. Ihm, *Phys. Rev. B* **65**, 085405 (2002).

<sup>33</sup>N. Troullier and J.L. Martins, *Phys. Rev. B* **43**, 1993 (1991).

<sup>34</sup>S. Iijima, T. Ichihashi, and Y. Ando, *Nature (London)* **356**, 776 (1992).

<sup>35</sup>D.L. Carroll, P. Redlich, P.M. Ajayan, J.C. Charlier, X. Blase, A. De Vita, and R. Car, *Phys. Rev. Lett.* **78**, 2811 (1997).

<sup>36</sup>C. Kim, B. Kim, S.M. Lee, C. Jo, and Y.H. Lee, *Appl. Phys. Lett.*

- 79**, 1187 (2001); Phys. Rev. B **65**, 165418 (2002).
- <sup>37</sup>Y.H. Lee, S.G. Kim, and D. Tománek, Phys. Rev. Lett. **78**, 2393 (1997); Chem. Phys. Lett. **265**, 667 (1997).
- <sup>38</sup>M. Fujita, K. Wakabayashi, K. Nakada, and K. Kusakabe, J. Phys. Soc. Jpn. **65**, 1920 (1996); K. Wakabayashi, M. Fujita, H. Ajiki, and M. Sigrist, Phys. Rev. B **59**, 8271 (1999); S. Ryu and Y. Hatsugai, *ibid.* **67**, 165410 (2003).
- <sup>39</sup>J.W. Mintmire, B.I. Dunlap, and C.T. White, Phys. Rev. Lett. **68**, 631 (1992).
- <sup>40</sup>Y. Saito, K. Hamaguchi, S. Uemura, K. Uchida, Y. Tasaka, F. Ikazaki, M. Yumura, A. Kasuya, and Y. Nishina, Appl. Phys. A: Mater. Sci. Process. **67**, 95 (1998).
- <sup>41</sup>A.G. Rinzler, J.H. Hafner, P. Nikolaev, L. Lou, S.G. Kim, D. Tománek, P. Nordlander, D.T. Colbert, and R.E. Smalley, Science **269**, 1550 (1995).
- <sup>42</sup>S.B. Fagan, A.J.R. da Silva, R. Mota, R.J. Baierle, and A. Fazzio, Phys. Rev. B **67**, 033405 (2003).